International Journal of Fluid Machinery and Systems
Vol. 8, No. 4, October-December 2015

DOI: http://dx.doi.org/10.5293/IJFMS.2015.8.4.304
ISSN (Online):1882-9554

**Original Paper**

# Numerical simulation of slit wall effect on the Taylor vortex flow with radial temperature gradient

**Dong Liu [1]，Chang-qing Chao [1]， Fang-neng Zhu [1] ，Xi-qiang Han [2]，Cheng Tang [1]**

[1]School of Energy and Power Engineering
Jiangsu University, Zhenjiang , 212013, China
[2]Beijing Shenwu Environment & Energy Technology Co.，Ltd
Beijing, 102200, China

**Abstract**

Numerical simulation was applied to investigate the Taylor vortex flow inside the concentric cylinders with a constant radial temperature gradient. The reliability of numerical simulation method was verified by the experimental results of PIV. The radial velocity and temperature distribution in plain and 12-slit model at different axial locations were compared, and the heat flux distributions along the inner cylinder wall at different work conditions were obtained. In the plain model, the average surface heat flux of inner cylinder increased with the inner cylinder rotation speed. In slit model, the slit wall significantly changed the distribution of flow field and temperature in the annulus gap, and the radial flow was strengthen obviously , which promoted the heat transfer process at the same working condition.

**Keywords**: Taylor vortex flow, Slit wall, temperature gradient, heat transfer, numerical simulation

## 1. Introduction

In 1923, Taylor[1] discovered the secondary flow existed in the annulus gap between two relatively rotating concentric cylinders, which is called Taylor-Couette flow. Since then, a lot of scholars carried out in-depth research on it.

Yang[2] studied the transition process of Taylor-Couette flow by flow visualization method, the aluminum particles were added to investigate the stability of flow field, they found as the rotation speed increased, the aluminum particles have the axial motion before the transition to Taylor vortex flow. Kedia et al.[3] studied the effects of heat transfer on Taylor-Couette flow, and found the heat transfer decreased with Grashof number in axisymmetric Taylor vortex flow regime, and increased with Grashof number after the flow becomes non-axisymmetric. Lee and Minkowycz [4] studied heat transfer characteristics by using the naphthalene sublimation technique in the annular gap between two short concentric cylinders which had either two plain walls or one plain and one axially slit wall, and yielded qualitative information regarding heat transfer but did not address the flow phenomena inside the annular gap. Liu[5] studied the axial wall slits effect on the Taylor vortex flow in the gap between two concentric cylinders by Particle Image Velocimetry, and found the existence of slit wall accelerated the transition process.

The above studies were done by experimental method. Many scholars have applied numerical simulation to the study of Taylor-Couette flow. Hayase [6] used numerical simulation to study the heat transfer process between rotating coaxial cylinders with periodically embedded cavities, and found the flow in a cavity interacted with Taylor vortices in the annular space to enhance heat transfer. Kang et.al[7] studied the temperature gradient effect on the circular-Couette flow, and found the vortex size increased as the Richardson number increased. Poncet et.al [8] applied Reynolds stress model to study heated Taylor-Couette flow with an axial Poiseuille flow, and provided the correlations for the averaged Nusselt number along both cylinders according to the flow control parameters Reynolds number and Prandtl number.

From the above studies, many scholars have studied the heat transfer effect on Taylor-Couette flow by experimental and numerical simulation method, some of them studied the wall geometry effect on the heat transfer ability, but little study about the slit wall effect on the Taylor vortex flow regime with radial temperature gradient. We have studied the slit wall effect on the flow stability and transition process [9,10], and based on these research works, we study a constant temperature gradient effect on Taylor vortex flow in the plain and slit wall models by numerical simulation, which is rarely reported in the previous studies.

Received September 14 2014; revised May 15 2015; accepted for publication August 20 2015: Review conducted by Kwang-Yong Kim.PhD. (Paper number O14027K)
Corresponding author: Dong Liu, Associate Professor, liudong@ujs.edu.cn

## 2. Computational domain and Numerical method

### 2.1 Computational domain

The geometries model used in this study is shown in Fig. 1. Radius of the inner cylinder is $r_i$=33mm，radius of the outer cylinder is $r_o$=40mm，the annular gap ($d$) between the inner and outer cylinders is 7mm and the length of the cylinders (L) is 336mm. In addition, the silt number of the slit model considered in this study is 12, the depth and width of each slit is 5mm, all the slits are mounted uniformly in the inner wall of outer cylinder. The geometry of plain and slit model is shown in Fig. 2.

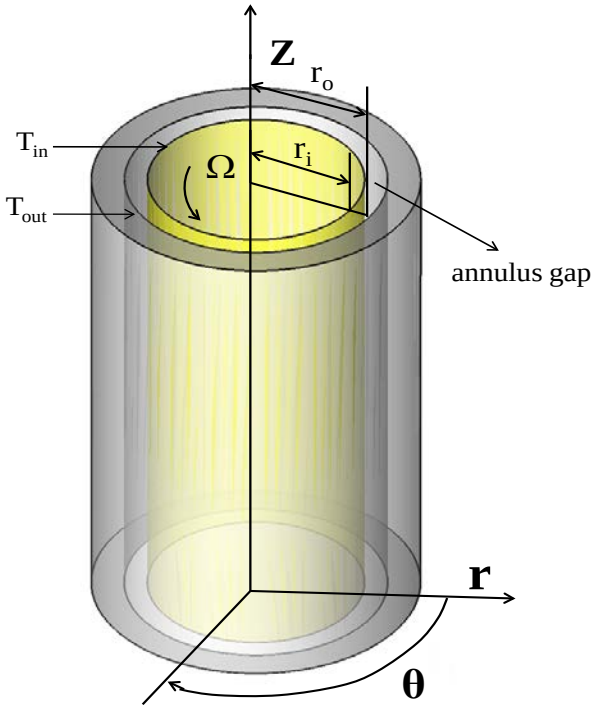


Fig.1 Schematic representation of the Taylor–Couette configuration with relevant notations

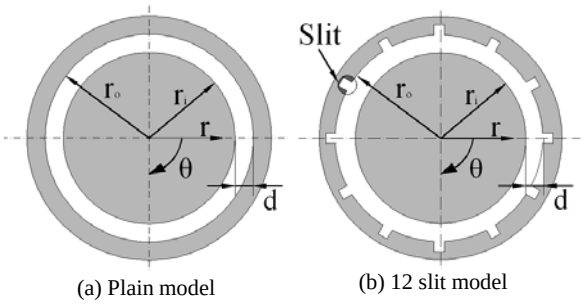


(a) Plain model (b) 12 slit model

Fig.2 Geometries of calculation models

Mesh independence study is conducted to verify the effect of density on the final simulation results. Structured hexahedral mesh is selected，which is more computational efficient and also convenient for the present domain. For the plain model, it is observed that a structured mesh with 250x30x330 grid points (along the circumferential, radial, and axial directions) is enough to provide the mesh independent results. The total mesh number is 2,475,000. For slit model, the grid scheme in the annulus gap is the same as plain model, in the slit region, the grid number along radial and circumferential direction is 10. The total mesh number in 12-slit model is 2,871,000.

### 2.2 Governing equation

The fluid is assumed to be incompressible and Newtonian. The governing equations for the fluid motion are the equation of continuity [11]

$$\frac{\partial \rho}{\partial t}+\frac{\partial}{\partial x_i}(\rho u_i)=0 \tag{1}$$

and momentum conservation equation

$$\frac{\partial}{\partial t}(\rho u_i)+\frac{\partial}{\partial x_j}(\rho u_i u_j)=-\frac{\partial p}{\partial x_i}+\frac{\partial \tau_{ij}}{\partial x_j}+\rho g_i+F_i \tag{2}$$

where p is the static pressure, $t_{ij}$ is the stress tensor, and $\rho g_i$ and $F_i$ are the gravitational body force and external body forces respectively.

The stress tensor $t_{ij}$ is given by

$$\tau_{ij}=\left[\mu\left(\frac{\partial u_i}{\partial x_j}+\frac{\partial u_j}{\partial x_i}\right)\right]-\frac{2}{3}\mu\frac{\partial u_l}{\partial x_l}\delta_{ij} \tag{3}$$

The energy conservation equation is given by

$$\frac{\partial \rho T}{\partial t}+\frac{\partial(\rho u_x T)}{\partial x}+\frac{\partial(\rho u_y T)}{\partial y}+\frac{\partial(\rho u_z T)}{\partial z}=\frac{\partial}{\partial x}(\frac{k}{C_P}\frac{\partial T}{\partial x})+\frac{\partial}{\partial y}(\frac{k}{C_P}\frac{\partial T}{\partial Y})+\frac{\partial}{\partial z}(\frac{k}{C_P}\frac{\partial T}{\partial z})+S_T \quad (4)$$

where $\rho$ is density of fluid, T is the temperature, $k$ is the thermal conductivity, $c_p$ is the specific heat of fluid at constant pressure.

### 2.3 Boundary conditions and numerical method

The outer cylinder with the surface temperature 24°C is resting, and the inner cylinder with surface temperature 25.2°C is rotating, $\Delta T$ is defined as ($T_{in}$ – $T_{out}$), $\Delta T$ =1.2° C. The effect of the temperature gradient is parameterized by the Grashof number, which is defined as $Gr = d^3\beta g\Delta T/\nu^2$, where g is the acceleration due to gravity, the thermal expansion coefficient $\beta$ is 0.00057 1/k, the kinematic viscosity $\nu$ is 1.52cSt, the density of the working fluid is 1780 kg/m$^3$, the specific heat capacity and the thermal conductivity of the working fluid is 2725J/kg·k, 0.209w/m.k respectively. So the Grashof number considered in this study is 1000 and Pr number is 35.6. Reynolds number is defined as $\mathrm{Re} = r_i d\Omega/\nu$ , where Ω is the angular velocity of the inner cylinder. Three different angular velocity is studied, which is 0.7567rad/s, 0.7896rad/s, and 0.8159rad/s, the corresponding Reynolds number is 115, 120, and 124 respectively.

Commercial software FLUENT 13 is used to solve this laminar flow. The solver is pressure-based and transient. The viscous model is laminar. The boussinesq assumption is adopted to consider the effect of natural convection. Under-relaxation factors are 0.3 for pressure, 0.7 for momentum, and 0.9 for energy. The discretization mode is second order for pressure, SIMPLEC for pressure-velocity coupling, second order upwind for momentum, and second order upwind for energy. The solution is computed from inner cylinder, and all initial values are zero unless specified. All the convergence criterions are 0.0001.

## 3. Results and Discussion

### 3.1 Numerical Validity

Figure 3 shows the velocity field in radial-axial plane of plain model, which is obtained by PIV measurement and numerical calculation at Re=115, the working condition in experimental work [10] is the same as that of numerical calculation. In this figure, the axial position, $Z^*=z/d$, and the radial position, $R^*=r/d$, are normalized by the annulus gap width. From Fig.3, it is found the flow characteristic in PIV and CFD result is consistent. To verify the accuracy of numerical calculation further, the radial velocity distribution at location R*=0.5 is extracted from numerical simulation and experimental results, which is shown in Fig.4. The difference of flow regime and velocity distribution between CFD and experimental results is small, which proves the numerical simulation method used in this paper is reliable.

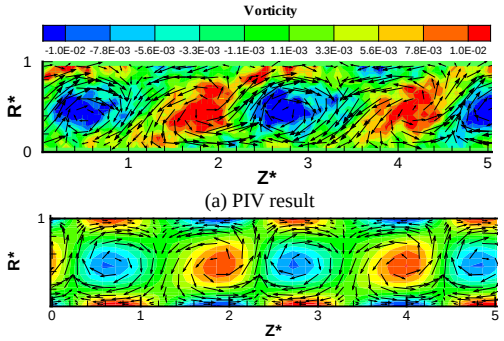


(a) PIV result

(b) CFD result

Fig.3 Velocity vectors and vortex contours on an R-Z plane at Re=115

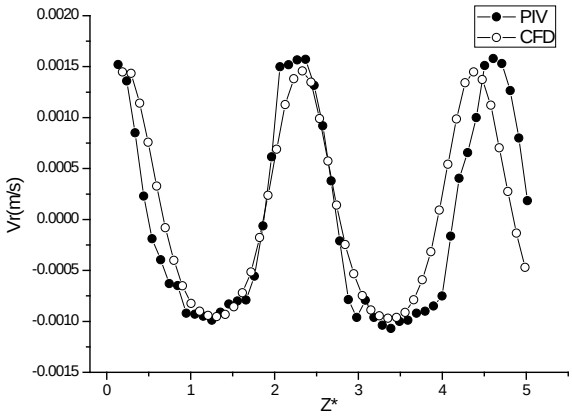


Fig.4 Distribution of the radial velocity component along an axial line through the center of the annular gap

### 3.2 Velocity and temperature distribution in plain model

Figure 5 shows velocity field in R-Z plane, the background presents the temperature distribution, the blue color represents lower temperature and the red one represents higher one. It is found the area between the vortex pairs to the inner cylinder wall has bigger temperature gradient, and most of the low temperature region located at the space between the vortex pairs to the outer cylinder. Figure 6 shows the heat flux and temperature distribution along the inner cylinder surface. The location with the peak heat flux value, corresponding to the space between the vortex pairs to the inner cylinder wall, where the temperature of the fluid was lower than 297.5k.

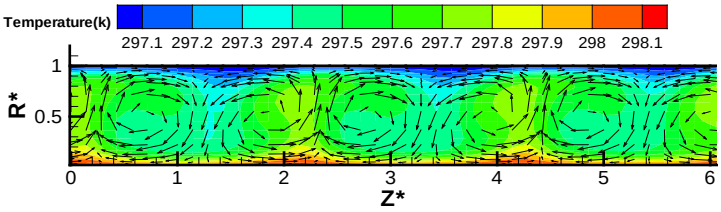


Fig.5 Velocity vectors and temperature contours on an R-Z plane at Re=115

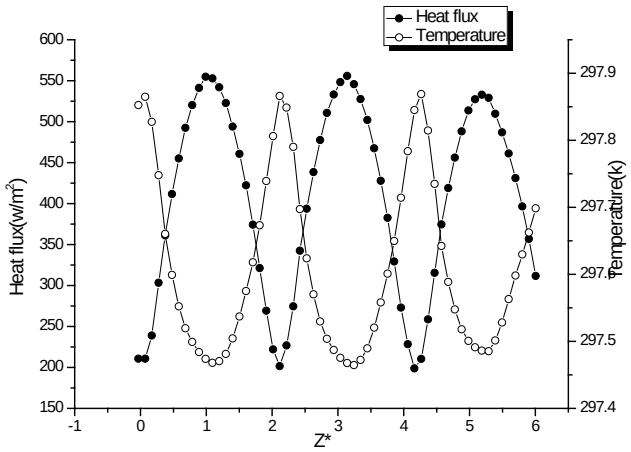


Fig.6 Distribution of Temperature and heat flux along an axial line through the center of the annular gap

Figure 7 shows the radial velocity distribution and temperature distribution along radial direction at different axial positions. The vortex center locates at the axial position of Z*=1.8 and Z*=2.8, the center position of two vortices in a vortex pair is Z*=2.3, the middle position of two vortex pairs is Z*=3.3. In Fig.7a, the radial velocity is quite small when Z* is 1.8 and 2.8. From inner cylinder to the outer one, radial velocity increases to the maximum valve at R*=0.5 and then decreases until R*=1 when Z* is 2.3 and 3.3. In Fig.7b, at each axial position, the temperature decreases from R*=0 to R*=0.2, and remains almost the same from R*=0.2 to R*=0.8 when Z* is 2.3 and 3.3. When Z* is 1.8 and 2.8, the temperature increases slightly until R*=0.7. When Z* is 3.3, the temperature gradient of the fluid to the inner cylinder wall is obviously larger than other positions, and the temperature gradient of the fluid to the outer cylinder wall is smaller than other positions. The main reason is that inflow radial velocity of the fluid at this position is larger, as the fluid moves toward the inner cylinder, the heat of the inner cylinder is taken away.

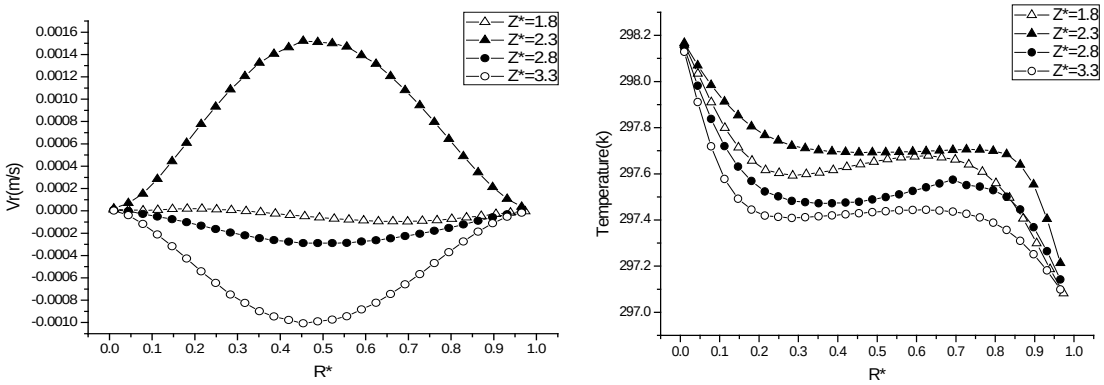


(a) Radial velocity distribution (b) Temperature distribution

Fig.7 Distribution of radial velocity and temperature along radial direction at different axial positions

Figure 8 shows the radial velocity distribution along axial direction at different Reynolds numbers. The maximum radial velocity increases by 26.7% when Re increases from 115 to 124, which indicates that the radial flow is intensified obviously as the Re increase.

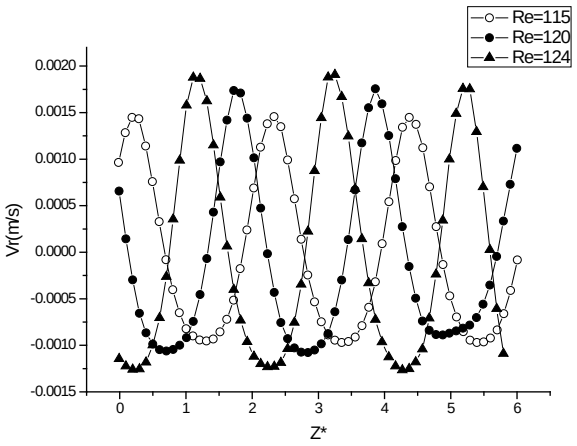


Fig.8 Distribution of radial velocity along axial direction for various Re

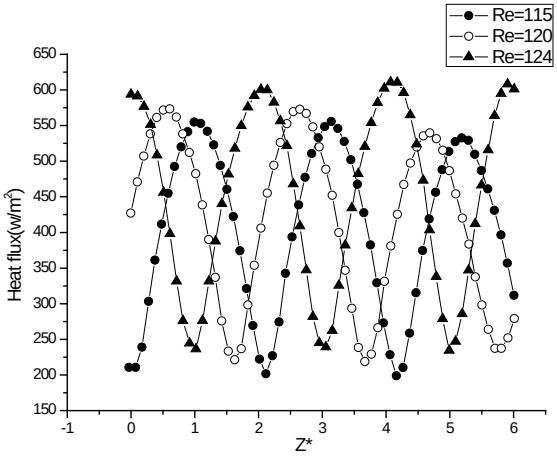


Fig.9 Distribution of heat flux along axial direction for various Re

Figure 9 shows the heat flux distribution along axial direction at different Re, it can be found the heat flux distribution has the periodic variation. As the increasing of the inner cylinder rotational speed, the heat transfer performance enhances obviously.

### 3.3 Velocity and temperature distributions in the slit model

Figure 10 shows velocity field of radial-axial plane in slit model, and the background represents the temperature distribution. Compared the temperature distribution in slit model with that in plain model, it is found the higher temperature area of fluid in slit model is smaller than that of plain model, and there is larger temperature gradient between the fluid area and the inner cylinder wall in slit model.

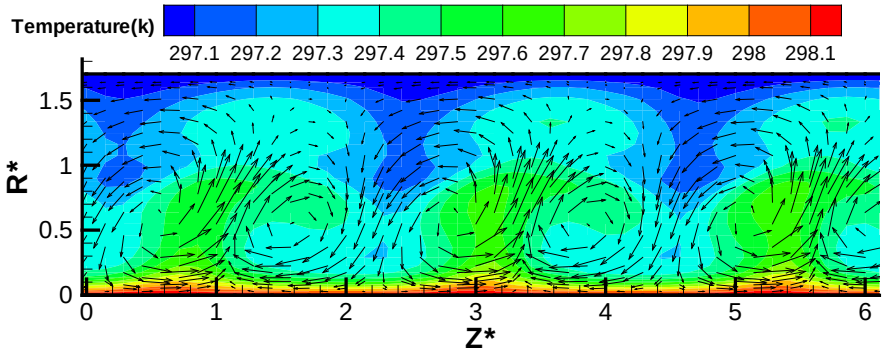


Fig.10 Velocity vectors and temperature contours on an r-z plane in 12-slit model

Figure 11 shows the temperature distribution along radial direction in plain and slit wall model at Re=115. It is found that the temperature gradient of the fluid to the inner cylinder wall in slit model is larger than that of plain model. When R* increases from 0.2 to 1.25, the temperature distribution in slit model has a fluctuation characteristics, and decreases rapidly as R* is larger than 1.25.

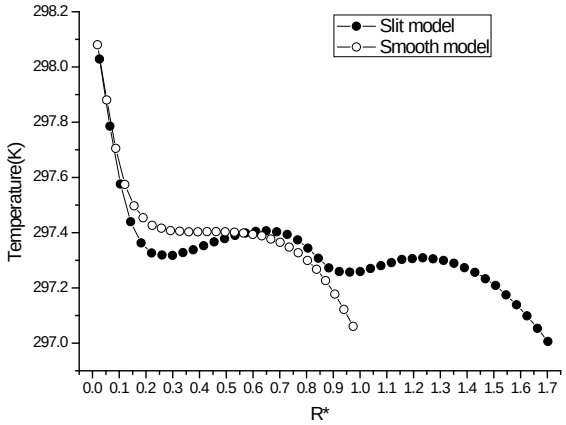


Fig.11 Distribution of temperature along radial direction in different models

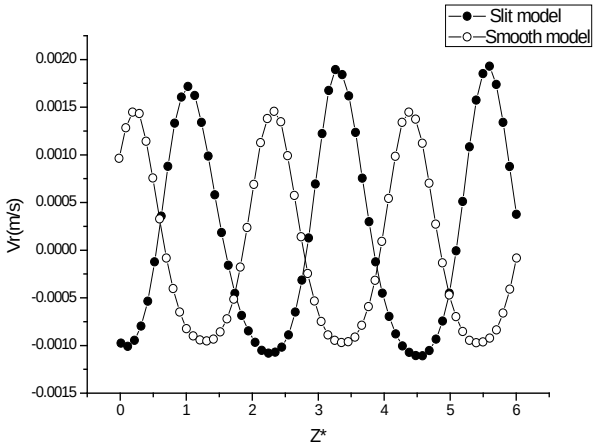


Fig.12 Distribution of radial velocity component along radial direction in different models

Figure 12 shows the radial velocity distribution along axial direction at Re=115. It is found that the maximum radial velocity in slit model is 32.2% larger than that of plain model, which indicates that the slit wall promotes the fluid in annulus gap to spread into slit space, and strengthened the radial flow [9]. The average surface heat flux on the inner cylinder of slit model increases by 10.6% compared to that of plain model at the same Re. In conclusion, the existence of slit wall enhances the average surface heat flux, and promotes the heat transfer performance because the radial flow is strengthen.

## 4. Conclusion

In this paper, Taylor vortex flow with radial temperature gradient in plain and slit wall models is studied by numerical simulation. The following conclusion is obtained by comparing the results of different models. As the increasing of the inner cylinder rotational speed, the radial outflow is intensified, and the heat transfer performance becomes better. The slit wall affects the flow filed in the annulus gap, which strengthens the radial flow, and as a result the heat transfer ability is better than plain model at the same working condition.

## Acknowledgments

This work was supported by National Natural Science Foundations of China (51206062), Six talent peaks project in Jiangsu Province (2014-ZBZZ-016), Jiangsu Planned Projects for Postdoctoral Research Funds(1302093C) and China Postdoctoral Science Foundation(2013M540420), also supported by Research Foundation for Advanced Talents of Jiangsu university(Grant No. 10JDG119) and the Priority Academic Program Development of Jiangsu Higher Education Institutions.

## References

[1] Taylor, G. I., 1923, “Stability of a viscous liquid contained between two rotating cylinders,” Philosophical Transactions of the Royal Society of London. Series A, Containing Papers of a Mathematical or Physical Character, Vol. 223, pp. 289-343.
[2] Yang, W. M. 2010, “Transformational phenomenon in the field of Taylor-Couette flow,” Experimental Techniques, Vol. 34, No. 6, pp. 42-48.
[3] Kedia, R., Hunt, M. L., and Colonius, T., 1998, “Numerical Simulations of Heat Transfer in Taylor-Couette Flow,” Journal of heat transfer, Vol. 120, No. 1, pp. 65-71.
[4] Lee, Y. N., and Minkowycz, W. J., 1989, “Heat transfer characteristics of the annulus of two-coaxial cylinders with one cylinder rotating,” International journal of heat and mass transfer, Vol. 32, No.4, pp. 711-722.

[5] Liu, D., Yang, X. Y., and Ding, J., 2012, “Axial Wall Slits Effect on the Helical Flow in the Gap between two Concentric Cylinders,” International Journal of Fluid Machinery and Systems, Vol.5, No.2, pp. 60-64.
[6] Hayase, T., Humphrey, J. A. C., and Greif R., 1992, “Numerical calculation of convective heat transfer between rotating coaxial cylinders with periodically embedded cavities,” Journal of Heat Transfer, Vol.114, No.3. pp. 589-597.
[7] Kang, C. W., Yang, K. S., and Mutabazi, I., 2009, “The effect of radial temperature gradient on the circular-Couette flow,” Journal of computational fluids engineering, Vol.14, No.3, pp. 16–24.
[8] Poncet, S., Haddadi, S., and Viazzo, S. 2011, “Numerical modeling of fluid flow and heat transfer in a narrow Taylor-Couette-Poiseuille system,” International Journal of Heat and Fluid Flow, Vol.32, No.1, pp. 128-144.
[9] Liu, D., Zhu J., and Wang, Y. Z. et al., 2014, “Numerical Simulation of the slit wall effect on flow stability in Taylor Vortex Flow Regime,” Journal of Drainage and Irrigation Machinery Engineering, Vol.32, No.3, pp. 1-5.
[10] Liu,D., Lee,S. H., and Kim, H. B., 2010, “Effect of a constant radial temperature gradient on a Taylor-Couette with axial wall slits,” Fluid Dynamics Research, Vol.42, No.6:065501.
[11] Kumar, M. A., and Prasad, B. V., 2012, “Computational investigations of impingement heat transfer on an effused concave surface,” International Journal of Fluid Machinery and Systems, Vol.5, No.2. pp. 72-90.